

Finite-Element Analysis of Dielectric Coated Antenna

N.BAMBA, S.GOTOH, S.ARAI, K.KAWAHATA, T.OKADA and M.MATSUHARA*

Murata Manufacturing Co.,Ltd.,Nagaokakyo,Kyoto,617 Japan

*Faculty of Engineering,Osaka University,Suita,Osaka,565 Japan

1. INTRODUCTION

Dielectric material can shorten a wire antenna in terms of wavelength reduction effect for electromagnetic waves. In the design of an antenna a simulation using a computer is a powerful tool. For a dielectric antenna, some methods have been proposed. J.H.Richmond and E.H.Newman calculated admittance characteristics for a wire antenna covered with a dielectric shell using a moment method[1]. However, their method is inadequate to calculate for the thicker dielectric shell and for dielectric material with high permittivity.

For a dielectric antenna using high permittivity material we expanded a simulation method proposed by A.Maruta and M.Matsuhara[2], so that an antenna problem can be handled. This method is based on Finite-Element Method(FEM). In general, FEM has an advantage that can calculate the electromagnetic field including the dielectric structures which is not restricted in shape and in permittivity. However, FEM is weak in antenna problem because of difficulty in setting boundary conditions. In order to overcome this problem, virtual boundaries that surround an antenna are placed. On the boundary the inner electromagnetic field obtained by FEM are connected with the outer one expressed with eigen modes in the free space. Using the eigen mode function as a weight function, these fields are connected by the Galerkin method.

In this paper, after the explanation of this method the comparison between the calculated and measured results on input return loss of an antenna are described.

2. THEORY

The theoretical explanation is presented for an antenna with symmetrical axis shown in Figure 1. Virtual boundaries that surround an antenna are placed. S_1 is the boundary between the antenna region and the coaxial cable, and S_2 is the boundary between the antenna region and the free space. In the inner region, Eq.(1) is derived from Maxwell equations by using the Galerkin method.

$$\int_V [\omega^2 \mu \mathbf{F}_m \cdot \mathbf{H} - \frac{1}{\epsilon} (\nabla \times \mathbf{F}_m) \cdot (\nabla \times \mathbf{H})] dV - \int_{S_1} (\mathbf{n} \times \mathbf{F}_m) \cdot (\frac{1}{\epsilon_1} \nabla \times \mathbf{H}_1) dS + \int_{S_2} (\mathbf{n} \times \mathbf{F}_m) \cdot (\frac{1}{\epsilon_2} \nabla \times \mathbf{H}_2) dS = 0 \quad (1)$$

Where \mathbf{H}_1 and \mathbf{H}_2 are magnetic field in the coaxial cable and the free space, respectively. By using weight function \mathbf{F}_m magnetic field \mathbf{H} in the inner region is expanded as:

$$\mathbf{H} = \sum_m \mathbf{F}_m \phi_m \quad , \quad (2)$$

where ϕ_m is an expansion coefficient. Here we considered only TM_{0kj} , where k

and j are wave numbers.

From continuity of magnetic field \mathbf{H} at the boundaries we get

$$\int_{S_1} \left(\frac{1}{\epsilon_1} \nabla \times \mathbf{P}_n \right) \cdot (\mathbf{n} \times \mathbf{H} - \mathbf{n} \times \mathbf{H}_1) dS = 0, \quad (3)$$

$$\int_{S_2} \left(\frac{1}{\epsilon_2} \nabla \times \mathbf{Q}_1 \right) \cdot (\mathbf{n} \times \mathbf{H} - \mathbf{n} \times \mathbf{H}_2) dS = 0, \quad (4)$$

where \mathbf{P}_n is an eigen mode function in the coaxial cable. \mathbf{Q}_1 is a mode function in the free space. Both \mathbf{P}_n and \mathbf{Q}_1 are weight functions.

\mathbf{H}_1 and \mathbf{H}_2 are expanded as follows:

$$\mathbf{H}_1 = \sum_n [a_n + b_n \exp(2j\beta_n z)] \mathbf{P}_n, \quad (5)$$

$$\mathbf{H}_2 = \sum_l c_l \mathbf{Q}_l, \quad (6)$$

where a_n , b_n and c_l are amplitude of incident waves, reflection waves and radiation waves, respectively.

Substituting Eqs.(2),(5) and (6) into Eqs. (1),(3) and (4), we obtain algebraic linear equations. The radiational characteristics and the reflection coefficient are obtained by solving these equations.

3. COMPARISON BETWEEN COMPUTATIONS AND MEASUREMENT RESULTS

SIMPLE DIELECTRIC COATED MONOPOLE ANTENNA

The calculated results obtained by the FEM mentioned above are compared with the measured one. A cross section for a dielectric coated monopole antenna handled here is shown in Figure 2. The dielectric cylinder with a hollow consists of dielectric ceramics, have a radiator electrode on the interior wall and is mounted on a square ground plane (100×100mm) for measurements. Infinite ground plane is assumed for calculations. Measurements and calculations are performed for five conditions in cylinder size. The inner diameter (d_{in}) varies from 1.6mm to 4.8mm, and the other parameters are fixed as shown in Figure 2. The center conductor of the connector is connected to the radiator electrode by solder.

Figure 3 shows the measured and calculated resonant frequency(f_0) which are plotted versus inner diameter d_{in} . Here it can be seen that both the measured and calculated f_0 increase with increasing d_{in} . This tendency relate to the fact that the wavelength reduction effect decrease with decreasing the volume of the dielectric cylinder. The difference between the calculated and measured results for each d_{in} is within 5%.

Figure 4 shows the measured and calculated input return loss which are plotted versus frequency for the case $d_{in}=3.2\text{mm}$. The calculated bandwidth (VSWR<3) is 4.7% and the measured one is 6.0%. It is supposed that this discrepancy between them results from the fact that our model for calculations does not include dielectric and conducting loss.

Though the calculated bandwidth is slightly smaller than the measured one, the good agreement between the calculated and measured f_0 in Figure 3 illustrates the ability of the method to treat geometries including dielectric

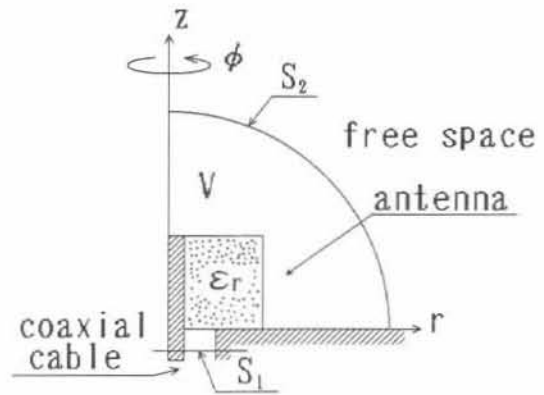


Figure 1 Geometry of an antenna with a symmetrical axis

materials with high permittivity.

DIELECTRIC COATED ANTENNA WITH A GROOVE

Consider a more complicated dielectric coated antenna which has a rectangular groove around the outside surface of the dielectric cylinder with a hollow. Figure 5 shows a cross section for the antenna measured and calculated here. The physical parameter is shown in the figure. Calculations and measurements are carried out for dielectric cylinder with $\epsilon_r=90$ and groove depth(x) from 0 to 4.0mm. The size of the ground plane used is 900x900mm.

The measured and calculated f_0 are compared in Figure 6. It can be seen that the f_0 increase almost linearly with increasing x. The measured f_0 are about 3% greater than the calculated one. It may results from the displacement of the dielectric cylinders from the center of the coaxial cable.

In Figure 7 the measured and calculated bandwidth (VSWR<3) are compared. The calculated bandwidth are slightly greater than the measured one, and the both results show the same tendency to increase bandwidth with increasing x. This discrepancy seems to be caused by dielectric and conducting loss mentioned above.

Considering that strictly speaking there are some differences between the model of calculations and the actual antenna, the calculated results shows good agreement with the measured one.

4. CONCLUSION

An advantage of the method presented here is to be able to treat an axially symmetric antenna with an arbitrary shape and with high permittivity. It is found that this simulation method has enough accuracy to estimate resonant frequency and bandwidth.

For the future, we plan to design a small and wide bandwidth dielectric coated antenna using this method.

REFERENCES

- [1] J.H.Richmond and E.H.Newman: "Dielectric coated wire antenna", Radio Sci.,11,pp.13-20(1976).
- [2] A.Maruta and M.Matsuhara: "Finite-Element Analysis of Waveguide Transfer Problem -Field Connection by Using the Galerkin Method-", IEICE,J72-C-I, 10,pp.577-582(1989).

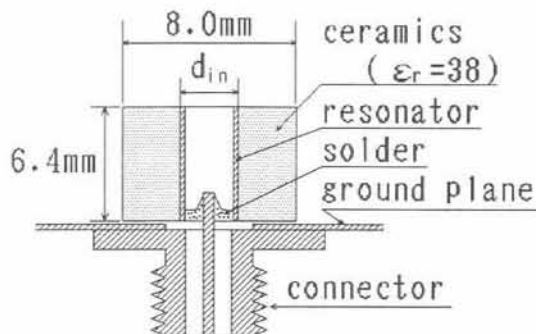


Figure 2 A cross section of the dielectric coated antenna

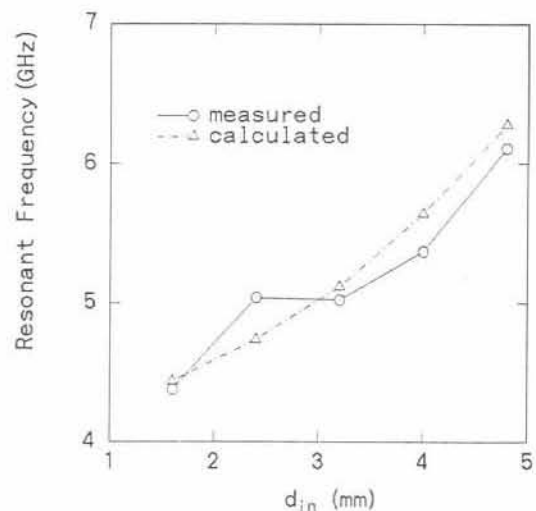


Figure 3 Comparison of the calculated and measured resonant frequencies

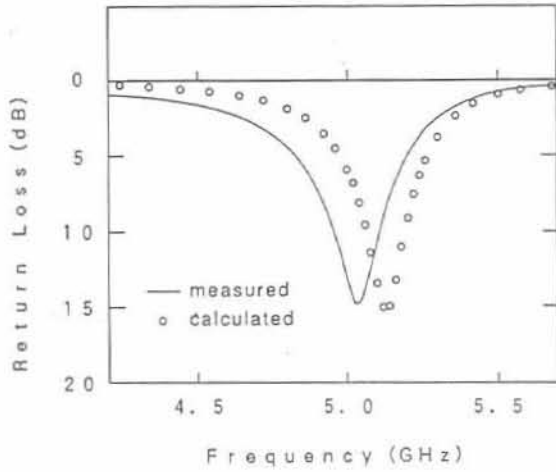


Figure 4 Return loss of the dielectric coated monopole antenna ($d_{in}=3.2\text{mm}$) plotted versus frequency

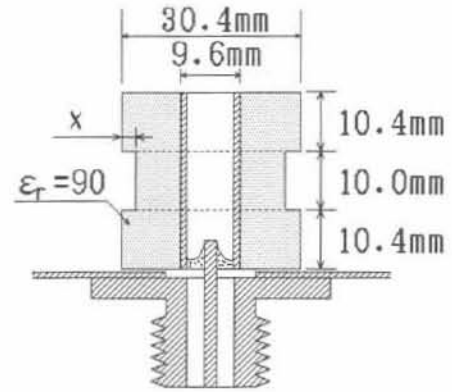


Figure 5 A cross section of the dielectric coated antenna with a groove

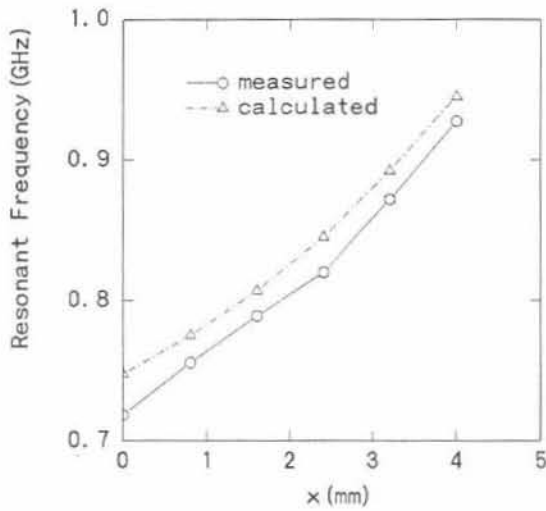


Figure 6 Resonant frequencies for dielectric monopole antenna with a groove

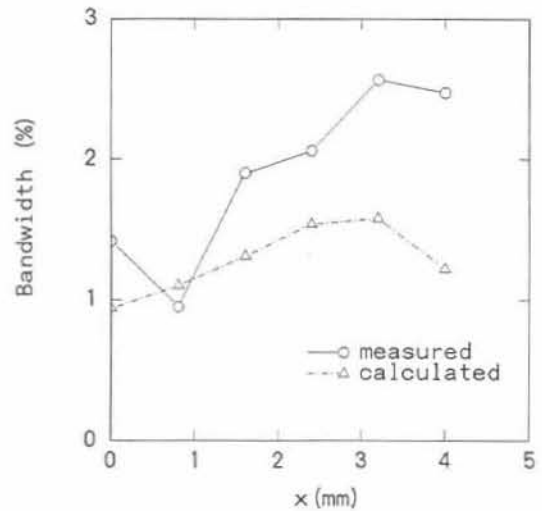


Figure 7 Bandwidth for dielectric monopole antenna with a groove plotted versus x